Graphene-based Plasmonic Phase Modulator for Terahertz-band Communication

Prateek K. Singh[1], **Gregory Aizin**[2], **Ngwe Thawdar**[3], **Michael Medley**[3] and **Josep Miquel Jornet**[1]

[1]Department of Electrical Engineering, University at Buffalo, The State University of New York, Buffalo, NY 14260, USA, E-mail: {prateekk,jmjornet}@buffalo.edu

[2]Department of Physical Sciences, Kingsborough Community College, Brooklyn, NY 11235, USA, E-mail: gregory.aizin@kbcc.cuny.edu

[3]Air Force Research Laboratory/RITE, Rome, NY 13441, USA, Email: {ngwe.thawdar,michael.medley}@us.af.mil

***Abstract*—In this paper, a graphene-based plasmonic phase modulator for Terahertz band (0.1–10 THz) communication is proposed, modeled and analyzed. The modulator is based on a fixed-length graphene-based plasmonic waveguide, and leverages the possibility to tune the propagation speed of Surface Plasmon Polariton (SPP) waves on graphene by modifying the Fermi energy of the graphene layer. An analytical model for the modulator is developed starting from the dynamic complex conductivity of graphene and a revised dispersion equation for SPP waves in gated graphene structures. By utilizing the model, the performance of the modulator is analyzed in terms of symbol error rate when utilized to implement a M-ary digital phase shift keying modulation. The model is validated by means of electromagnetic simulations, and numerical results are provided to illustrate the performance of the modulator.**

***Index Terms*—Phase Modulation, Graphene, Plasmonics, Terahertz Band**

I. Introduction

Wireless data rates have doubled every eighteen months for the last three decades. Following this trend, Terabit-per-second (Tbps) links are expected to become a reality within the next five years. The limited available bandwidth for communication systems in the microwave frequency range motivates the exploration of higher frequency bands for communication. In this direction, millimeter wave (mm-wave) communication systems, such as those at 60 GHz [1], have been heavily explored in the last decade. However, despite their much higher operation frequency, the available bandwidth for communication is less than 10 GHz. This would require the use of communication schemes able to provide a spectral efficiency in the order of 100 bits/second/Hz to support 1 Tbps, which is several times above the state-of-the-art for wireless communication.

In this context, the Terahertz band (0.1–10 THz) is envisioned as a key player to satisfy the need for much higher wireless data rates [2], [3]. Despite the absorption from water vapor molecules, the THz band supports very large transmission bandwidths, which range from almost 10 THz for communication distances below one meter, to multiple transmission windows, each of them tens to hundreds of GHz wide, for distances in the order of tens of meters. Traditionally, the lack of compact and efficient THz signal sources and detectors, able to operate at room temperature, has limited the use of the THz band. However, major progress in the last decade [4], [5] is finally helping to close the THz gap.

In addition to THz signal sources and detectors, a modulator is needed to embed information on the transmitted signals. The desired properties of a modulator include high modulation bandwidth, i.e., the speed at which the properties of the modulated signal can be changed, and high modulation depth, i.e., the maximum difference between modulation states. Different types of modulators able to control the amplitude or phase of THz waves have been developed to date [6]. In [7], a high-electron-mobility transistor based on a III-V semiconductor material was utilized to modulate the amplitude of a THz wave. In [8], a metamaterial-based modulator was utilized to control the phase of a THz wave. In both cases, sub-GHz modulation bandwidths and low modulation depths limit the use of these devices in practical communication systems.

More recently, the use of graphene to develop THz wave modulators has been proposed [9]. Graphene has excellent electrical conductivity, making it very well suited for propagating extremely-high-frequency electrical signals [10]. In [11], a graphene-based amplitude modulator for THz waves was developed. This was enabled by the possibility to dynamically control the conductivity of graphene. In [12], a similar principle was exploited in a graphene-based meta-device. In these setups, the main challenge is to increase the modulation depth. A low modulation depth makes the transmitted symbols more difficult to distinguish and, thus, results in higher symbol error rates (SER) in practical communication systems.

In this paper, we propose, model and analyze the performance of a graphene-based plasmonic phase modulator for THz-band communications. The proposed modulator consists of a fixed-length graphene-based plasmonic waveguide with a metallic back gate. Its working principle relies on the possibil-

Acknowledgement of Support and Disclaimer: (a) The State University of New York at Buffalo acknowledges the U.S. Government's support in the publication of this paper. This material is based upon work funded by AFRL, under AFRL Grant No. FA8750-15-1-0050. (b) Any opinions, findings and conclusions or recommendations expressed in this material are those of the author(s) and do not necessarily reflect the views of AFRL.

Approved for Public Release; Distribution Unlimited: 88ABW-2015-5986.

ity to electronically control the propagation speed of a Surface Plasmon Polariton (SPP) wave on graphene at THz frequencies by modifying the chemical potential of the graphene layer. Starting from the dynamic complex conductivity of graphene and a revised dispersion equation for SPP waves (Sec. II), we develop an analytical model for the plasmonic phase modulator (Sec. III). By utilizing the model, we analyze the performance of the proposed plasmonic modulator when utilized to implement a M-ary phase shift keying modulation in terms of SER (Sec. IV). We validate the model by means of electromagnetic simulations, and provide numerical results to illustrate the modulator performance (Sec. V).

II. Propagation Properties of Surface Plasmon Polariton Waves on Gated Graphene Structures

The analysis of the proposed plasmonic phase modulator requires the characterization of the SPP propagation properties on graphene. These depend on the conductivity of the graphene sheet. In this section, we first recall the conductivity model utilized in our analysis and then define the dispersion equation for SPP waves on gated graphene structures.

A. Complex Conductivity Model of Graphene

In our analysis, we consider a surface conductivity model for infinitely large graphene sheets obtained using the Kubo formalism [13], [14]. This is given by

$$\sigma^g = \sigma^g_{\text{intra}} + \sigma^g_{\text{inter}}, \tag{1}$$

$$\sigma^g_{\text{intra}} = i\frac{2e^2}{\pi\hbar^2}\frac{k_B T}{\omega + i\tau_g^{-1}} \ln\left(2\cosh\left(\frac{E_F}{2k_B T}\right)\right), \tag{2}$$

$$\sigma^g_{\text{inter}} = \frac{e^2}{4\hbar}\left(H\left(\frac{\omega}{2}\right) + \mathrm{i}\frac{4\omega}{\pi}\int_0^\infty \frac{G(\epsilon) - G(\omega/2)}{\omega^2 - 4\epsilon^2}\, d\epsilon\right), \tag{3}$$

and

$$G(a) = \frac{\sinh(\hbar a/k_B T)}{\cosh(E_F/k_B T) + \cosh(\hbar a/k_B T)}, \tag{4}$$

where $\omega = 2\pi f$, $\hbar = h/2\pi$ is the reduced Planck's constant, e is the electron charge, k_B is the Boltzmann constant, T is temperature, E_F refers to the Fermi energy of the graphene sheet, and τ_g is the relaxation time of electrons in graphene, which depends on the electron mobility μ_g. E_F can be easily modified by means of electrostatic bias or gating of the graphene layer, enabling the aforementioned antenna tuning.

As we showed in [15], a more accurate conductivity model can be developed by taking into account the impact of electron lateral confinement on graphene nano-ribbons, but the two models converge for graphene strips which are 50 nm wide or more. In our analysis, we consider plasmonic resonant cavities which are a few hundred nanometers wide. Finally, from [13], [14], it is important to note that the conductivity model described by (1) and the following was derived by neglecting the spatial dispersion of the AC field. Therefore, it can be used for the analysis of the SPP propagation in the long wavelength limit only, i.e., $\omega \gg k_{spp} v_F$, where k_{spp} is the SPP wave number and $v_F \approx 8 \times 10^5$ m/s is the Fermi velocity of Dirac fermions in graphene.

B. Dispersion Equation for Surface Plasmon Polariton Waves

The propagation properties of SPP waves can be obtained by deriving and solving the SPP wave dispersion equation on graphene. In many of the related graphene plasmonic works [16], [17], [18], the dispersion equation was obtained by considering a graphene layer at the interface between two infinitely large dielectric materials, usually between air and silicon dioxide (SiO_2). However, the proposed modulator relies on the presence of a metallic ground plane at a distance d from the graphene layer, which is needed both to create the plasmonic waveguide as well as to control the Fermi energy of the graphene layer and tune its conductivity.

From [19], the dispersion equation for Transverse Magnetic (TM) SPP waves on gated graphene structures in the quasi-static regime—i.e., for $k_{spp} \gg \omega/c$, where c is the speed of light—is given by

$$-i\frac{\sigma^g}{\omega\varepsilon_0} = \frac{\varepsilon_1 + \varepsilon_2 \coth(k_{spp} d)}{k_{spp}}, \tag{5}$$

where σ^g is the conductivity of graphene given by (1), ε_1 is the relative permittivity of the dielectric above the graphene layer, and ε_2 is the relative permittivity of the dielectric between the graphene layer and the metallic ground plane, which are separated by a distance d. It can be easily shown by taking the limit of $d \to \infty$ that (5) tends to the quasi-static dispersion equation of SPP waves in ungated graphene used in the aforementioned works.

By solving (5), the complex wave vector k_{spp} can be obtained. The real part of the wave vector,

$$\mathrm{Re}\{k_{spp}\} = \frac{2\pi}{\lambda_{spp}} = \frac{\omega}{v_p}, \tag{6}$$

determines the SPP wavelength λ_{spp} and the SPP wave propagation speed. The imaginary part determines the SPP decay or, inversely,

$$\mathcal{L} = \frac{1}{2\,\mathrm{Im}\{k_{spp}\}}, \tag{7}$$

determines the SPP propagation length, which is defined as the distance at which the SPP intensity has decreased by a value of $1/e$. Unfortunately, a closed-form expression for k_{spp} in this case does not exist, but can only be obtained numerically.

III. Graphene-based Plasmonic Phase Modulator

In this section, we explain the working principle of the plasmonic phase modulator and develop its analytical model.

A. Working Principle

The conceptual design of the proposed graphene-based plasmonic phase modulator is shown in Fig. 1. The phase modulator consists of a plasmonic waveguide, which is composed of a graphene sheet (the plasmonic material) mounted over a metallic flat surface (the ground plane), with a dielectric material layer in between, which supports the graphene layer. In this paper, we consider that a SPP wave is already propagating over the graphene layer. Different mechanisms could be utilized to launch the SPP wave. For example, a THz plasma wave could be generated by a HEMT-like device and coupled to the

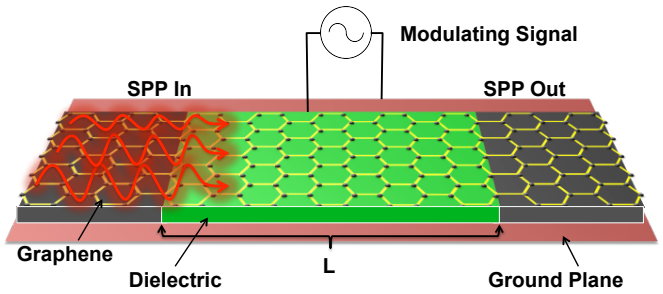

Fig. 1. Graphene-based plasmonic phase modulator.

graphene waveguide [20]. Alternatively, a Quantum Cascade Laser and a grating structure could be utilized for the same [5].

The basic idea for any phase modulator is to establish a relation between the data bits to be transmitted, which constitute the modulating signal, and the transmitted signal phase. In our proposed plasmonic phase modulator, the modulating signal is applied as a bias voltage to the graphene layer and controls its Fermi energy, E_F. From (6), (5) and (1), it is clear that the Fermi energy directly controls the propagation speed of the SPP wave on the gated graphene structure. Therefore, for a fixed length waveguide, the phase at the output of the waveguide is effectively modulated by the data bits to be transmitted. The resulting signal can be further propagated and eventually radiated in free-space by means of a plasmonic nano-antenna [15], [17], [18].

B. Analytical Model

In this section we develop an analytical model for the phase of the plasmonic signal at the output of the plasmonic phase modulator shown in Fig. 1. We denote the plasmonic signals at the input and the output of the plasmonic waveguide as X and Y, respectively. The modulator frequency response is denoted by H. The following relation can be then written,

$$Y\left(f, E_F\right) = X\left(f\right) H\left(f, E_F\right), \tag{8}$$

where f stands for frequency and E_F is the Fermi energy of the graphene layer on which the SPP wave propagates.

The modulator frequency response H is given by

$$H\left(f, E_F\right) = \left|H\left(f, E_F\right)\right| \exp\left(j\theta\left(f, E_F\right)\right), \tag{9}$$

where $|H|$ accounts for the variation in the SPP wave intensity and θ represents the change in the SPP phase at the output of the fixed-length waveguide.

From Sec. II, the magnitude of the modulator response can be written as

$$\left|H\left(f, E_F\right)\right| = \exp\left(-2\,\mathrm{Im}\{k_{spp}\left(f, E_F\right)\}L\right), \tag{10}$$

where L represents the waveguide length.

The total phase change θ that the SPP wave suffers as it propagates through the waveguide is given by

$$\theta\left(f, E_F\right) = \frac{2\pi L}{\lambda_{spp}\left(f, Ef\right)} = L\,\mathrm{Re}\left\{k_{spp}\left(f, E_F\right)\right\}, \tag{11}$$

where λ_{spp} is the plasmonic wavelength obtained from k_{spp} as discussed in Sec. II, which depends on the signal frequency f and the Fermi energy E_F.

By combining (10) and (11) in (9), the modulator frequency response can be written as

$$\begin{aligned} H\left(f, E_F\right) = &\exp\left(-2\,\mathrm{Im}\left\{k_{spp}\left(f, E_F\right)\right\} L\right) \\ &\cdot \exp\left(j\,\mathrm{Re}\left\{k_{spp}\left(f, E_F\right)\right\} L\right). \end{aligned} \tag{12}$$

In an ideal phase modulator, the intensity or amplitude of the signal should remain constant, independently of the phase. However, the SPP decay in graphene structures is not negligible. As a result, we cannot independently modulate the signal amplitude and phase. This has a direct impact on the performance of the modulator in a practical communication system, which we analyze in the next section.

IV. Performance Analysis

In this section, we define the constellation of a non-uniform plasmonic phase shift keying digital modulation and formulate the SER for M-ary modulations.

A. Signal Space Constellation

The signal space or constellation represents the possible symbols generated by a given modulation scheme as points in the complex plane. The real part of each of such points is referred to as the in-phase component and the imaginary part denotes the quadrature component.

The number of modulated symbols or points in the constellation is given by $M = 2^k$, where $k = 2, 4, ...$ refers to the modulation order. The position of each symbol S_m, $m = 1..M$, depends on the modulator behavior. For the system described in Sec. III, at fixed carrier frequency f_c, the magnitude and phase of each symbol is given by

$$S_m = |S_m| \exp\left(\theta_m\right), \tag{13}$$

$$|S_m| = A_0 \left|H\left(f_c, E_{F,m}\right)\right|, \tag{14}$$

$$\theta_m = \theta_0 + \theta\left(f_c, E_{F,m}\right), \tag{15}$$

where A_0 and θ_0 refer to the amplitude and phase of the input SPP wave. $E_{F,m} = \{E_{F,1}, E_{F,2}, ...E_{F,M}\}$ is the set of Fermi energies that correspond to the transmitted symbols. In our analysis, we consider $A_0 = 1$ and $\theta_0 = 0$. The constellation for the proposed plasmonic phase modulator can only be numerically obtained and will be provided in Sec. V.

B. Symbol Error Rate

The most common metric for a modulation scheme in a practical communication system is the SER. This is implicitly related to the modulation intensity or depth. The more "distinguishable" the symbols are, the lower the SER. In general terms, for a modulated symbol S_m, the symbol error probability P_e is given by [21],

$$P_e = P\left\{\text{Detect } S_{\tilde{m}}, \tilde{m} \neq m \mid \text{Given that } S_m \text{ is sent}\right\}, \tag{16}$$

where $m = 1, 2, 3...M$. The SER for a digital phase modulation with uniform constellation is derived based on the symbol decision regions, which due to symmetry, are easy to define. However, this is not the case for non-uniform modulations.

Instead, the SER for the proposed plasmonic phase modulation scheme can be directly derived starting from the distance between symbols in the non-uniform constellation.

In general terms, the union bound for the SER is given by [21],

$$SER \leq \frac{1}{M} \sum_{m=1}^{M} \sum_{1 \leq \tilde{m} \leq M, \tilde{m} \neq m} Q \left[\sqrt{\frac{D(S_m, S_{\tilde{m}})^2}{2N_0}} \right], \quad (17)$$

where the Q function refers to the tail probability of the standard normal distribution, $D(S_m, S_{\tilde{m}})$ stands for the distance between two symbols S_m and $S_{\tilde{m}}$, and is given by

$$D(S_m, S_{\tilde{m}})^2 = \|S_m - S_{\tilde{m}}\|^2, \quad (18)$$

and N_0 is the noise power spectral density.

A common representation of the SER is as a function of signal-to-noise ratio (SNR) or the energy per symbol to noise power spectral density E_s/N_0. From (14), this is given by

$$SNR_m = \frac{E_{s,m}}{N_0} = \frac{|H_m(f_c, E_F)|^2}{N_0}. \quad (19)$$

Finally, by combining (17), (18) and (19), the SER for the non-uniform constellation can be further expressed as

$$SER \leq \frac{1}{M} \sum_{m=1}^{M} \sum_{1 \leq \tilde{m} \leq M, \tilde{m} \neq m} Q \left[\left(\frac{E_{s,m} e^{j2\theta_m}}{N_0} + \frac{E_{s,\tilde{m}} e^{j2\theta_{\tilde{m}}}}{N_0} - 2\cos(\theta_m + \theta_{\tilde{m}}) \sqrt{\frac{E_{s,m}}{N_0} \cdot \frac{E_{s,\tilde{m}}}{N_0}} \right)^{1/2} \right]. \quad (20)$$

The SER will be numerically investigated in the next section.

V. Simulation and Numerical Results

In this section, we validate our models and analyze the performance of the proposed plasmonic phase modulator.

A. Model Validation

We utilize COMSOL Multi-physics to simulate the behavior of the plasmonic phase modulator shown in Fig. 1. Graphene is modeled as a transition boundary condition with impedance given by (1), with $\tau_g = 2.2$ ps at room temperature $T = 300$ K. The graphene layer rests on top of a metallic ground plane with a 90 nm-thick SiO_2 dielectric in between ($\varepsilon_r = 4$). In Fig. 2, the z-component of the electric field on a 2-μm-long graphene-based waveguide is shown for f_c=4 THz and two values of E_F, namely, 0.13 eV and 0.28 eV. For E_F = 0.13 eV, the waveguide length L corresponds to approximately one and a half SPP wavelength and, thus, it introduces a phase change of π. For E_F = 0.28 eV, the waveguide length L corresponds to one full SPP wavelength and introduces a phase change of 2π. Hence, we can define a plasmonic phase modulator of order M=2, where bit "0" is transmitted as a phase change of 2π by tuning E_F to 0.28 eV and bit "1" is transmitted with a phase change of π by tuning E_F to 0.13 eV.

In addition to the phase, we are interested in the change in the amplitude of the SPP wave amplitude, as it will affect the signal space constellation and the SER. In Fig. 3(a)

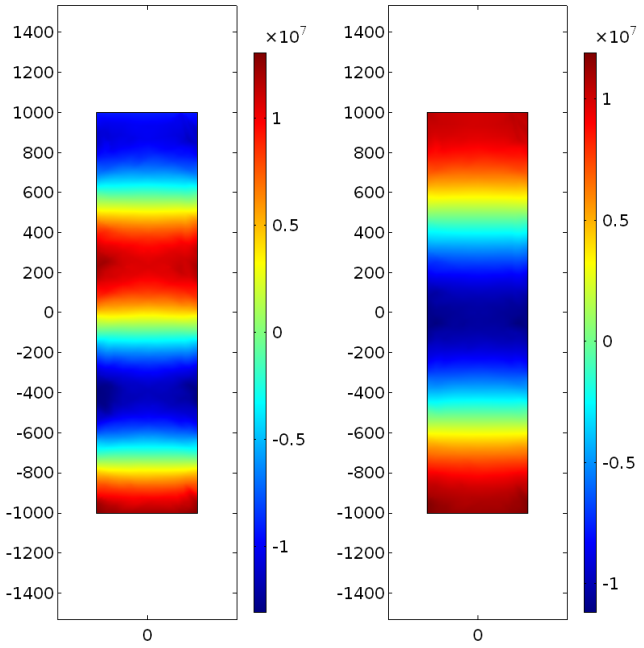

(a) $E_F = 0.13$ eV (b) $E_F = 0.28$ eV

Fig. 2. Electric field distribution over a graphene-based waveguide at f_c=4 THz, for different Fermi energies, E_F (L=2 μm, d=90 nm).

and Fig. 3(b), we illustrate the magnitude and phase of the plasmonic phase modulator as a function of the Fermi energy, E_F, and for different carrier frequencies, f_c. On the one hand, we are interested in working in a range of E_F such that the magnitude of the modulator does not significantly change. On the other hand, however, we need at least a phase difference of π to create orthogonal symbols. Next, we investigate the performance of a specific modulator design.

B. Constellation and Symbol Error Rate

In Fig. 4(a), the non-uniform constellation for a plasmonic phase modulator with $f_c = 4$ THz, $E_{F,0} = 0.28$ eV, $E_{F,1} = 0.13$ eV, and $L = 2$ μm, $d = 90$ nm is shown. Similarly, in Fig. 4(b), the SER (17) for the proposed modulator is shown as a function of the SNR and compared to that of a uniform binary phase shift keying (BPSK) modulation with the same average energy per symbol E_s. As expected, the SER for the proposed modulator is slightly higher but still comparable to that of the uniform case.

VI. Conclusions and Future Work

In this paper, we have proposed a novel graphene-based plasmonic phase modulator scheme for THz-band communication. The proposed modulator leverages the possibility to tune the propagation speed and, thus, output phase of a SPP wave as its propagates over a graphene layer. We have developed an analytical model for the modulator by starting from the surface conductivity model of graphene and the dispersion equation of SPP waves in gated graphene structures. COMSOL Multi-physics has been utilized to validate the proposed model. We have then analyzed the performance of plasmonic modulator in terms of symbol error rate for the specific case of a digital binary phase shift keying modulation. The results have

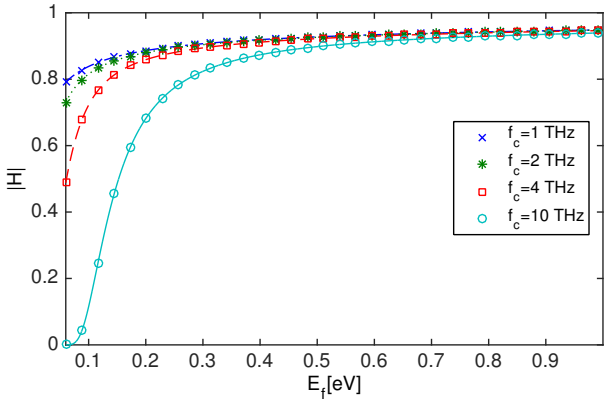

(a) Magnitude, $|H(f_c, E_F)|$

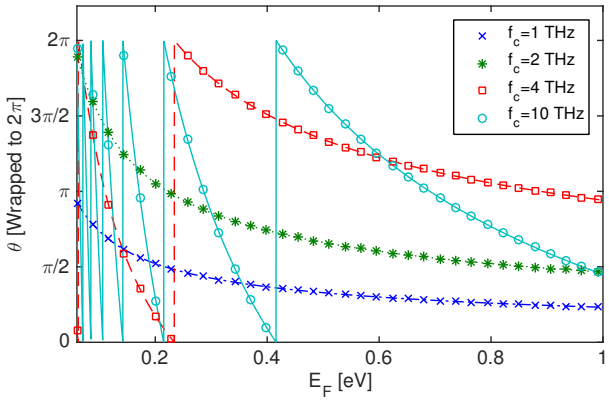

(b) Phase, $\theta(f_c, E_F)$

Fig. 3. Frequency response of the phase modulator, as a function of the Fermi energy, E_F, for different carrier frequencies f_c (L=2 μm, d=90 nm).

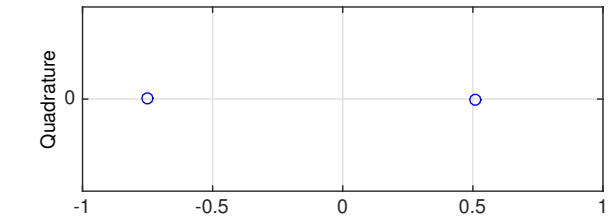

(a) Constellation

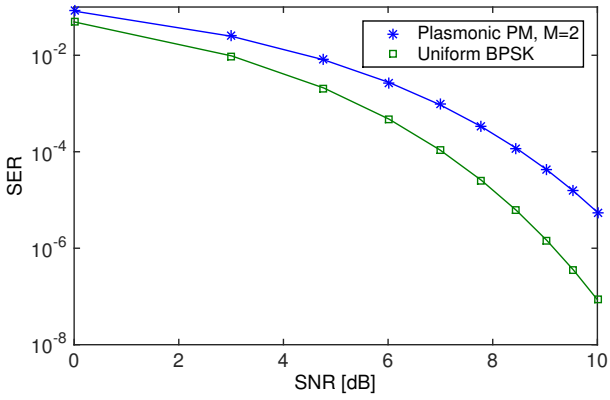

(b) SER

Fig. 4. Performance of a binary plasmonic phase modulator with $E_{F,0} = 0.28$ eV, $E_{F,1} = 0.13$ eV, (f_c=4 THz, L=2 μm, d=90 nm).

shown that, despite generating a non-uniform signal space constellation, the modulated symbols are sufficiently apart to be easily distinguishable. This highlights the potential of the proposed approach to enable practical wireless communication systems in the THz band.

REFERENCES

[1] T. Rappaport, J. Murdock, and F. Gutierrez, "State of the art in 60-ghz integrated circuits and systems for wireless communications," *Proceedings of the IEEE*, vol. 99, no. 8, pp. 1390 –1436, Aug. 2011.

[2] I. F. Akyildiz, J. M. Jornet, and C. Han, "Terahertz band: Next frontier for wireless communications," *Physical Communication (Elsevier) Journal*, vol. 12, pp. 16 – 32, Sep. 2014.

[3] T. Kurner and S. Priebe, "Towards THz Communications-Status in Research, Standardization and Regulation," *Journal of Infrared, Millimeter, and Terahertz Waves*, vol. 35, no. 1, pp. 53–62, 2014.

[4] V. Radisic, K. Leong, D. Scott, C. Monier, X. Mei, W. Deal, and A. Gutierrez-Aitken, "Sub-millimeter wave inp technologies and integration techniques," in *IEEE MTT-S International Microwave Symposium (IMS)*, May 2015, pp. 1–4.

[5] Q. Lu, S. Slivken, N. Bandyopadhyay, Y. Bai, and M. Razeghi, "Widely tunable room temperature semiconductor terahertz source," *Applied Physics Letters*, vol. 105, no. 20, p. 201102, 2014.

[6] M. Rahm, J.-S. Li, and W. J. Padilla, "Thz wave modulators: a brief review on different modulation techniques," *Journal of Infrared, Millimeter, and Terahertz Waves*, vol. 34, no. 1, pp. 1–27, 2013.

[7] T. Kleine-Ostmann, P. Dawson, K. Pierz, G. Hein, and M. Koch, "Room-temperature operation of an electrically driven terahertz modulator," *Applied physics letters*, vol. 84, no. 18, pp. 3555–3557, 2004.

[8] H.-T. Chen, W. J. Padilla, M. J. Cich, A. K. Azad, R. D. Averitt, and A. J. Taylor, "A metamaterial solid-state terahertz phase modulator," *Nature Photonics*, vol. 3, no. 3, pp. 148–151, 2009.

[9] S. Luo, Y. Wang, X. Tong, and Z. Wang, "Graphene-based optical modulators," *Nanoscale Research Letters*, vol. 10, no. 1, pp. 1–11, 2015.

[10] A. C. Ferrari, F. Bonaccorso, V. Fal'Ko, K. S. Novoselov, S. Roche, P. Bøggild, S. Borini, F. H. Koppens, V. Palermo, N. Pugno *et al.*, "Science and technology roadmap for graphene, related two-dimensional crystals, and hybrid systems," *Nanoscale*, vol. 7, no. 11, pp. 4598–4810, 2015.

[11] B. Sensale-Rodriguez, R. Yan, M. M. Kelly, T. Fang, K. Tahy, W. S. Hwang, D. Jena, L. Liu, and H. G. Xing, "Broadband graphene terahertz modulators enabled by intraband transitions," *Nature Communications*, vol. 3, pp. 780+, Apr. 2012.

[12] S. H. Lee, H.-D. Kim, H. J. Choi, B. Kang, Y. R. Cho, and B. Min, "Broadband modulation of terahertz waves with non-resonant graphene meta-devices," *IEEE Transactions on Terahertz Science and Technology*, vol. 3, no. 6, pp. 764–771, 2013.

[13] L. Falkovsky and A. A. Varlamov, "Space-time dispersion of graphene conductivity," *The European Physical Journal B*, vol. 56, pp. 281–284, 2007.

[14] G. W. Hanson, "Dyadic Green's functions and guided surface waves for a surface conductivity model of graphene," *Journal of Applied Physics*, vol. 103, no. 6, p. 064302, 2008.

[15] J. M. Jornet and I. F. Akyildiz, "Graphene-based plasmonic nano-antenna for terahertz band communication in nanonetworks," *IEEE JSAC, Special Issue on Emerging Technologies for Communications*, vol. 12, no. 12, pp. 685–694, Dec. 2013.

[16] M. Jablan, H. Buljan, and M. Soljačić, "Plasmonics in graphene at infrared frequencies," *Physical Review B*, vol. 80, p. 245435, Dec. 2009.

[17] I. Llatser, C. Kremers, A. Cabellos-Aparicio, J. M. Jornet, E. Alarcon, and D. N. Chigrin, "Graphene-based nano-patch antenna for terahertz radiation," *Photonics and Nanostructures - Fundamentals and Applications*, vol. 10, no. 4, pp. 353–358, Oct. 2012.

[18] M. Tamagnone, J. S. Gomez-Diaz, J. R. Mosig, and J. Perruisseau-Carrier, "Reconfigurable terahertz plasmonic antenna concept using a graphene stack," *Applied Physics Letters*, vol. 101, no. 21, p. 214102, 2012.

[19] V. Ryzhii, "Terahertz plasma waves in gated graphene heterostructures," *Japanese journal of applied physics*, vol. 45, no. 9L, p. L923, 2006.

[20] J. M. Jornet and I. F. Akyildiz, "Graphene-based plasmonic nano-transceiver for terahertz band communication," in *Proc. of European Conference on Antennas and Propagation (EuCAP)*, 2014.

[21] J. G. Proakis and D. K. Manolakis, *Digital Signal Processing (4th Edition)*. Upper Saddle River, NJ, USA: Prentice-Hall, Inc., 2006.